



# Kent Academic Repository

Le, N.C.H., Gubala, V., Gandhiraman, R.P., Daniels, S. and Williams, D.E. (2011) *Evaluation of different nonspecific binding blocking agents deposited inside poly(methyl methacrylate) microfluidic flow-cells*. *Langmuir*, 27 (14). pp. 9043-9051. ISSN 0743-7463.

## Downloaded from

<https://kar.kent.ac.uk/45228/> The University of Kent's Academic Repository KAR

## The version of record is available from

<https://doi.org/10.1021/la2011502>

## This document version

Author's Accepted Manuscript

## DOI for this version

## Licence for this version

UNSPECIFIED

## Additional information

Unmapped bibliographic data:LA - English [Field not mapped to EPrints]J2 - Langmuir [Field not mapped to EPrints]C2 - 21648475 [Field not mapped to EPrints]AD - Biomedical Diagnostics Institute (BDI), Dublin City University, Dublin 9, Ireland [Field not mapped to EPrints]AD - National Centre for Plasma Science and Technology (NCPST), Dublin City University, Dublin 9, Ireland [Field not mapped to EPrints]AD - MacDiarmid Institute for Advanced Materials and Nanotechnology, Department of Chemistry, University of Auckland, Auckland-1142, New Zealand [Field not mapped to EPrints]AD - CSIRO Materials Science and Engineering, Hi...

## Versions of research works

### Versions of Record

If this version is the version of record, it is the same as the published version available on the publisher's web site. Cite as the published version.

### Author Accepted Manuscripts

If this document is identified as the Author Accepted Manuscript it is the version after peer review but before type setting, copy editing or publisher branding. Cite as Surname, Initial. (Year) 'Title of article'. To be published in *Title of Journal*, Volume and issue numbers [peer-reviewed accepted version]. Available at: DOI or URL (Accessed: date).

## Enquiries

If you have questions about this document contact [ResearchSupport@kent.ac.uk](mailto:ResearchSupport@kent.ac.uk). Please include the URL of the record in KAR. If you believe that your, or a third party's rights have been compromised through this document please see our [Take Down policy](https://www.kent.ac.uk/guides/kar-the-kent-academic-repository#policies) (available from <https://www.kent.ac.uk/guides/kar-the-kent-academic-repository#policies>).

# Evaluation of different non-specific binding blocking agents deposited inside poly(methyl methacrylate) (PMMA) microfluidic flow-cells

Nam Cao Hoai Le<sup>1\*,\*\*</sup>, Vladimir Gubala<sup>1</sup>, Ram P. Gandhiraman<sup>1</sup>, Stephen Daniels<sup>1,2</sup>, David E. Williams<sup>1,3</sup>

<sup>1</sup>Biomedical Diagnostics Institute (BDI), Dublin City University, Dublin 9, Republic of Ireland

\* Present address: CSIRO Materials Science and Engineering, Highett, Victoria 3190, Australia

<sup>2</sup>National Centre for Plasma Science and Technology (NCPST), Dublin City University, Dublin 9, Republic of Ireland

<sup>3</sup>MacDiarmid Institute for Advanced Materials and Nanotechnology, Department of Chemistry, University of Auckland, Auckland-1142, New Zealand

\*\* Corresponding author e-mail: nam.le@csiro.au

## Abstract

Poly(methyl methacrylate) (PMMA) flow-cells containing microwells were deposited with different non-specific binding blocking agents namely bovine serum albumin (BSA), cationic lipid (DOTAP) and diethylene glycol dimethyl ether (DEGDME). Water contact angle (WCA) and atomic force microscope (AFM) measurements were carried out to confirm the successful depositions of BSA, DOTAP, DEGDME onto the PMMA surfaces. Fluorescent intensity measurements were performed to evaluate the degree of non-specific adsorption of Cy5-labeled anti-IgG proteins onto plain and oxygen plasma treated (PT) PMMA flow-cells as well as PMMA flow-cells deposited with different above-mentioned blocking agents. We then employed a label-free detection method called total internal reflection ellipsometry (TIRE) to evaluate the stability of the deposited blocking agents inside the PMMA flow-cells. It was found that while DOTAP was the best agent for blocking the non-specific adsorption, it could be removed from the PMMA surfaces of the flow-cells upon rinsing with phosphate buffer saline (PBS) and later deposited back onto the Au-coated glass sensing substrate of the TIRE. The removal of the blocking agents from PMMA surfaces and their deposition onto the sensing substrate were further manifested by measuring the kinetics and the amount of adsorbed anti- $\alpha$ -hCG proteins. Overall, the dry DEGDME coating by plasma enhanced chemical vapor deposition (PECVD) showed very good blocking and excellent stability for subsequent assay inside the microwells. Our results could be useful when one considers what blocking agents should be used for PMMA-based microfluidic immunosensor or biosensor devices by looking at both the blocking efficiency and the stability of the blocking agent.

## 1. Introduction

Micro-total analysis systems ( $\mu$ -TAS), also called 'lab-on-a-chip', can acquire, separate, and analyze a variety of samples, and the micro-sizing and integration of these functions promises enormous medical and economic benefits [1-4]. Their small size, decreased analytical time and tiny sample consumption help to improve bioassay performance. Poly(methyl methacrylate) (PMMA) is an excellent polymer material to be employed in the manufacturing of low-cost  $\mu$ -TAS devices since they possess excellent optical, thermal, chemical and biocompatible properties. However, during the functioning of PMMA-based  $\mu$ -TAS devices, cells, proteins or oligonucleotides in solution are exposed to a large hydrophobic PMMA surface area. Accordingly, one of the biggest problem with PMMA-based  $\mu$ -TAS devices is that they could non-specifically absorb a large amounts of analytes [5-8]. For examples, in PMMA-based electrophoresis separation devices, the non-specific adsorption could result in band broadening, poor resolution, analytical irreproducibility and low separation efficiency. These are believed to be largely caused by the non-uniform electroosmotic flow due to the inhomogeneous zeta potential along the separation length of the PMMA devices fouled with non-specific proteins and DNA [6-9]. Furthermore, when highly-concentrated samples are used in these separation devices, this non-specific absorption may cause clogging of the devices [5]. For PMMA-based immunoassay and biosensor devices, when

low concentrations of samples are used there might not be enough analyte to reach other functional (i.e. sensing or detection) components of the devices, i.e. sample loss [5-7].

Numerous methods have been proposed to modify the surface of PMMA to reduce the non-specific adsorption of biomolecules [8]. The reported modification methods could be broadly categorized into dynamic coating and permanent modification by means of chemical reactions. Lin *et al.* [9] used dynamic coating technique to deposit PMMA channels with poly(ethyleneoxide) (PEO). A hybrid dynamic coating of *n*-dodecyl  $\beta$ -D- altoside (DDM) and methyl cellulose (MC) method has been developed by Dang *et al.* [10] to suppress analytes adsorption inside a PMMA microchannel. Similarly, Mohamadi *et al.* [11] reported a dynamic coating of methylcellulose (MC) and a nonionic detergent (polysorbate 20) onto PMMA channel also for suppressing the protein adsorption. On the other hand, permanent modification of PMMA surface by surface chemistry, mostly with PEG derivatives, has also been used to reduce the non-specific adsorption of analytes into the PMMA surfaces. Lai *et al.* [12] employed UV initiated polymerization technique to immobilize poly(hydroxyethyl methacrylate-co-ethylene glycol dimethacrylate) on the internal walls of the channels forming a monolithic stationary gel for an acrylamide separation of DNA. An atom-transfer radical polymerization method was developed by Bi *et al.* [7] to form poly(ethylene glycol dimethacrylate-co-methylether methacrylate) copolymer on the surface of PMMA chips for increasing the hydrophilicity and electrophoretic separation of proteins. A similar chemistry has been adopted by Liu *et al.* [13] to graft poly(ethylene glycol) (PEG) on the PMMA surface after the deposition of 2-Bromoisobutyryl bromide. The majority of these PMMA devices and their associated non-specific binding coatings are designed for electrophoresis and separation. Although, these above-mentioned modification methods have been successful in reducing the non-specific adsorption of the biomolecules onto the PMMA surfaces, to the best of our knowledge there has been no study on the stability of these coatings in contact with buffers and its effect on subsequent immunoassays performed on the PMMA devices integrated with a sensing element.

This paper reports a comprehensive comparison among different coatings for reducing non-specific adsorption on PMMA surface and the effect of the stability of the coatings with respect to the assays performed on a gold sensing element integrated inside a PMMA flow-cell. To this end, the PMMA surface of the flow-cells has been modified by dynamic coating with BSA and cationic lipid DOTAP, by wet chemical deposition of DEGDME and by plasma enhanced chemical vapour deposition (PECVD) of dry DEGDME. Water contact angle (WCA) and atomic force microscopy (AFM) were employed to confirm the successful surface modifications of the PMMA surface. Fluorescent intensity was measured inside the microwells of the PMMA flow-cells to evaluate the effectiveness of each coatings against the non-specific adsorption of Cy5-labeled anti-IgG. Finally, total internal reflection ellipsometry (TIRE) [14-21] with spectra and kinetic data of adsorption of anti- $\alpha$ -human chorionic gonadotropin (anti- $\alpha$ -hCG) was used to evaluate the stability of the coatings under buffer rinsing. Our results could be useful when choosing a blocking agent, its deposition and characteristics, for suppression of non-specific binding of biomolecules on a PMMA surface. In that regard, a good coating needs not only to effectively suppress the non-specific adsorption of biomolecules but also must show stability under prolonged rinsing and immersing with buffer which is commonly required in. This is believed to be useful for the design and development of PMMA-based microfluidic immunosensor and biosensors [22-26].

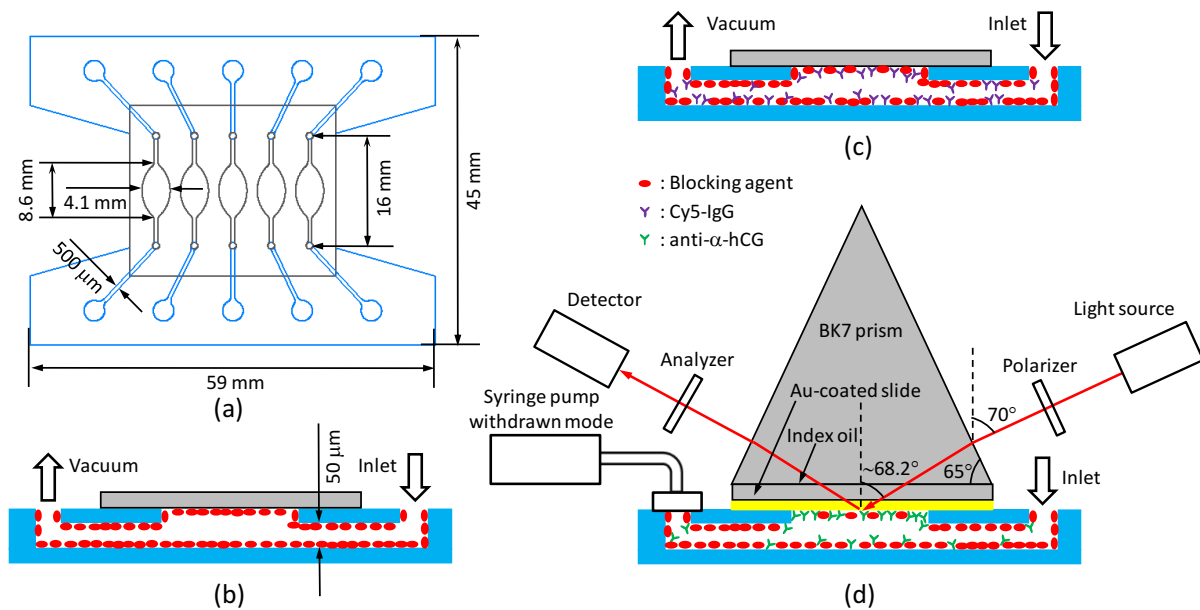


**Fig. 1.** (a) Top view of the PMMA flow-cell with five microwells, (b) cross-sectional view of one microwell of the PMMA flow-cell closed with a cyclo olefin polymer (COP) lid during the deposition of BSA, DOTAP or DEGDME by wet chemistry (c) cross-sectional view of the same microwell in (b) during the adsorption of Cy5-labelled anti-IgG for fluorescent measurements (d) TIRE experiment setup on a spectroscopic ellipsometry with a blocked PMMA microwell, a Au-coated glass slide, a BK7 prism, and a syringe pump.

## 2. Experimental

### 2.1 Materials

Cyclo olefin polymer (COP) slides (Zeonor® 1060R) (25 mm × 75 mm, 1 mm thick) were supplied by Åmic AB (Uppsala, Sweden). Polymethylmethacrylate (PMMA) sheets (0.25 mm thick, size 600 mm × 600 mm, impact modified) were supplied by Goodfellow Cambridge Limited (Huntingdon, England). Double-coated pressure sensitive adhesive (PSA) tapes (50 μm thick, AR8890) were purchased from Adhesives Research Ireland Ltd. (Limerick, Ireland). Gold-coated standard glass slides (Ti/Au = 2 nm/48 nm, 26 mm × 76 mm, 1 mm thick) were purchased from Phasis Sarl (Geneva, Switzerland). Transfection reagent I contains DOTAP:DOPE (1:1 w/w) was obtained from Avanti Polar Lipids, Inc. (Alabaster, AL, USA). Phosphate buffered saline (PBS, pH 7.4, 0.01 M), albumin from bovine serum (BSA, 98%), tetraethyl orthosilicate, 99.999% (TEOS, Si(OC<sub>2</sub>H<sub>5</sub>)<sub>4</sub>), diethylene glycol dimethyl ether (DEGDME, CH<sub>3</sub>O(CH<sub>2</sub>CH<sub>2</sub>O)<sub>2</sub>CH<sub>3</sub>) were all purchased from Sigma Aldrich (Dublin, Ireland). All chemicals were used as received without further purification. The Cy5-labelled anti-human IgG was purchased from Molecular Probes™ (Eugene, OR). The anti-α-human chorionic gonadotropin (anti-α-hCG) (clone 3299:4) was kindly donated by Inverness Medical Innovations (Bedford, UK).

### 2.2 Deposition of blocking agents into PMMA microfluidic flow-cells

The five-microwell flow-cell, containing four layers, was fabricated in poly(methyl methacrylate) (PMMA) and pressure-sensitive adhesive (PSA) using a CO<sub>2</sub> ablation laser machining system (**Fig 1(a)**). The fabrication method of the PMMA flow-cell has been reported elsewhere [21]. For deposition of BSA and DOTAP, a standard COP slide was glue to the top PSA layer of a PMMA flow-cell to form a close channel as shown in **Fig 1(b)**. 50 μl of BSA 1wt% in PBS and 50 μl of 50 mM DOTAP in DI water was deposited at two inlets of two nearby microwells of a half of the flow-cell. Vacuum was applied at the outlets of the two microwells to withdraw the liquid into the microwells. The solutions of BSA and DOTAP were allowed to adsorb to the PMMA microwell for 60 min and rinsed by 50 μl of PBS twice and dried with nitrogen [27-30]. Another flow-cell was oxygen plasma treated in 5 min and closed with a COP slide before 50 μl of 50 mM DEGDME was

applied with the same fashion as of BSA and DOTAP. The DEGDME solution was also allowed to react for 60 min before being rinsed by 50  $\mu$ l PBS twice and dried with nitrogen. For deposition of dry DEGDME by PECVD, the open PMMA flow-cell was subjected to plasma cleaning and activation in an argon plus oxygen mixed plasma, with a flow rate of 100 standard cubic centimetre per minute (sccm) of argon and oxygen, for 1 min at 100 W and then the DEGDME deposition was carried out by sequential deposition of tetraethylorthosilicate (TEOS) and diethylene glycol dimethyl ether (DEGDME) by low pressure Plasma Enhanced Chemical Vapor Deposition (PECVD) [31-33]. The flow of TEOS and DEGDME were controlled using needle valve and the deposition was carried out in an argon plasma. The details about the PECVD chamber can be found elsewhere [34]. All the depositions mentioned above were repeated on flat PMMA sheets for water contact angle (WCA) and atomic force microscopy (AFM) measurements.

### 2.3 Water contact angle

The wettability of different deposited films on PMMA sheets were analyzed by measuring the water contact angle (WCA) of the surfaces using the First Ten Angstroms FTA200 (Portsmouth, VA) contact angle analyser. In order to guarantee the flatness of the PMMA sheets, they were glued to PSA layers on top of glass slides before measurements. A high purity HPLC grade water (Sigma Aldrich, Dublin, Ireland) is used for the measurement. The water contact angle of each deposited films were measured three times at three locations on the PMMA sheets.

### 2.4 Atomic force microscopy

Atomic force microscopy (AFM) was used to compare the topographical surface created by the various surface modification processes. Similar to WCA measurements, the PMMA sheets were also glued to PSA layers on top of glass slides before AFM measurements. A Digital Instruments (DI) BioScope™ II (Veeco Instruments Inc., Plainview, NY, USA) operating in contact mode under ambient conditions was used. Images were acquired with a silicon tip mounted on a silicon nitride cantilever (Veeco Probes, Camarillo, CA, USA) with a spring constant of 0.06 N/m operating at a resonant frequency from 12 to 24 kHz and at a scan rate of 0.25 Hz. Coated surfaces were analyzed over 5  $\mu$ m  $\times$  5  $\mu$ m sample areas at a resolution of 256  $\times$  256 pixels and images were produced using Research NanoScope 7.30 software (Veeco Instruments Inc., Plainview, NY, USA). Zero-order plane fitting was used to remove the image bow that can result from the scanner moving out of plane with the sample.

### 2.5 Fluorescent microscopy

After the deposition of the blocking agents, the COP lids of the PMMA flow-cells were replaced with new COP lids since the PSA layer still maintain its adherence toward COP several times. For plain, plasma treated (PT) and dry DEGDME, the COP lids were applied to the PSA layer for the first time to form a closed channel. 30  $\mu$ l of 25  $\mu$ g/ml of Cy5-IgG in PBS (pH 7.4) was applied in each microwell of the PMMA flow-cell using vacuum and allowed to react for 1 h before being rinsed by PBS and dried with nitrogen. The COP lids were removed from the PMMA flow-cell before observation with fluorescent microscope. An inverted fluorescence microscope (IX81, Olympus Co., Japan) equipped with an EMCCD camera (DV887-BI, Andor Technology, UK) cooled to 0 °C and an MT20 fluorescence illumination unit fitted with a 150 W Xenon lamp was used in combination with a MCy5 filter set to image the fluorescence of the Cy5-labelled anti-IgG proteins. The fluorescence inside the microwells of the flow-cell was obtained using a UPlanSApo objective lens, 4 $\times$ , NA 0.16 (Olympus Co., Japan). The fluorescent images were acquired using the Cell<sup>^</sup>R software (Olympus Soft Imaging Solutions GmbH, Germany). All fluorescent images were acquired using the same set of parameters (exposure time of 330 ms, lamp power of 77.9%, EM gain of 94, resolution of 512  $\times$  512 pixels (2.048  $\times$  2.048 mm<sup>2</sup>)). The fluorescence intensity was quantified using Wasabi software (ver 1.50, Hamamatsu Photonics Germany GmbH, Germany) in a rectangular area of 500  $\mu$ m  $\times$  1000  $\mu$ m in each image captured.

### 2.6 Total internal reflection ellipsometry

The TIRE experimental setup was based on the UVISEL spectroscopic ellipsometer (Jobin Yvon Horiba, France) (Fig. 1(d)) [21]. The Au-coated glass sensing substrate was first glued to the PMMA flow-cell by

adhesion of the PSA reaction microwell layer. A BK7 prism was placed on top of the sensing substrate with an intermediate refractive index matching oil and secured by tapes (**Fig. 1(d)**). A syringe pump (Harvard Apparatus, Boston, USA) was connected to the outlet of one microwell of the flow-cell through a polymer tubing and a PDMS connector for performing one assay at a time. Two modes of measurements were carried out with TIRE: kinetic and spectral measurement. In both modes, the  $\Psi$  and  $\Delta$  values defined by the ratio  $\rho$  of the reflection coefficients  $R_p$  and  $R_s$  for components of light polarized parallel  $-p$  and perpendicular  $-s$  to the plane of incidence following the ellipsometry equation were measured [15].

A droplet of PBS buffer was injected at the inlet of the microwell and was withdrawn into the microwell by the syringe pump operating under the withdrawn mode. New droplets of PBS buffers were injected at the same inlet when the previous droplet was nearly emptied. The flow rate of the syringe pump was set at 5  $\mu\text{l}/\text{min}$  for a period of 15 min. Afterwards, the first set of  $\Psi$  and  $\Delta$  spectra were recorded at an angle of incidence of  $70^\circ$  with wavelengths ranging from 400 nm to 850 nm. The integration time was 200 ms and the spectral resolution was 2 nm. After the first  $\Psi$  and  $\Delta$  spectra were recorded, the kinetic measurement mode were turned on at a fixed wavelength, i.e. around 3 nm shift from the surface plasmon resonance (SPR) wavelength obtained from the first  $\Psi$  spectrum of the first spectra [17-18]. The integration time and interval in kinetic mode were set at 100 ms and 100 ms, respectively. The syringe pump was operated again at flow rate of 5  $\mu\text{l}/\text{min}$  after the inlet of the microwell was deposited with a droplet of anti- $\alpha$ -hCG 50  $\mu\text{g}/\text{ml}$  in PBS buffer (pH 7.4). New droplets were injected for a total period the kinetic measurement of 60 min. The kinetic mode was turned off and the spectral mode was restarted to measure the second  $\Psi$  and  $\Delta$  spectra corresponding to the adsorption of anti- $\alpha$ -hCG to the Au-coated glass surface. Although the flow-cell contains five microwells, only one assay was performed at a time on one microwell to prevent any possible shifting of the light rays in the optical setup. PsiDelta 2 software (Jobin Yvon Horiba, France) was used for fitting the data from the measured  $\Psi$  and  $\Delta$  spectra from TIRE. A four-layer model similar to the model used in [16, 18, 21] was used in the fitting to estimate the thickness of the organic layer first deposited onto the Au surface and then the thickness of anti- $\alpha$ -hCG.

### 3. Results and discussion

#### 3.1 Deposition of blocking agents onto PMMA surfaces

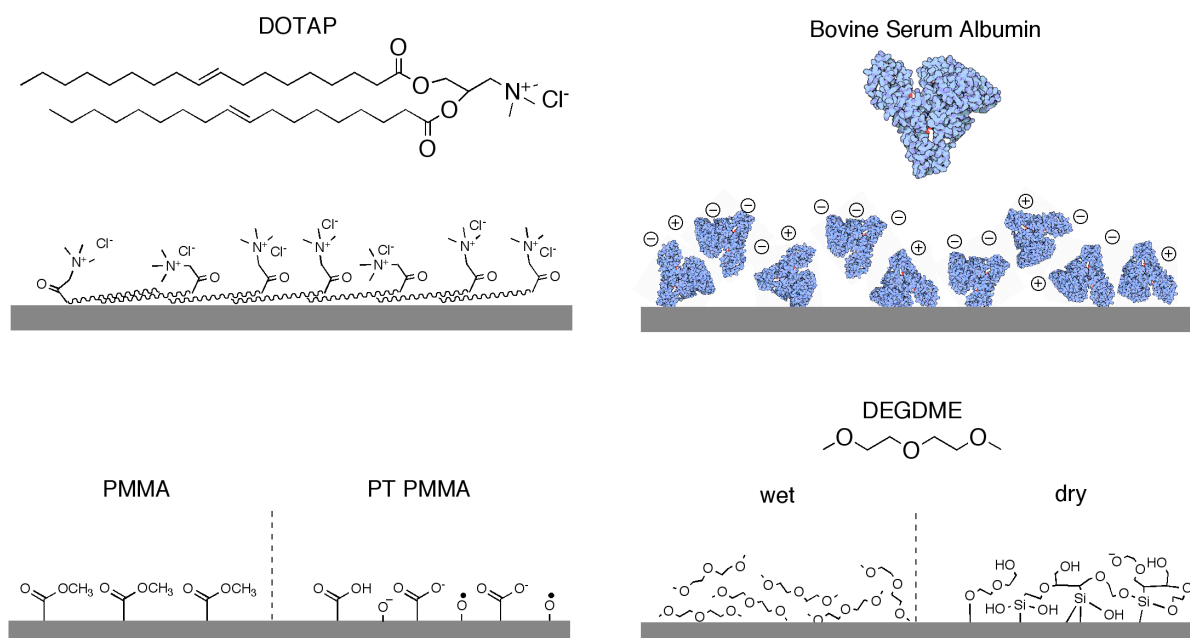


**Fig. 2.** A schematic illustrating the nature of the chemical groups present on the PMMA surface after treating the pristine PMMA with DOTAP, BSA, plasma and DEGDME (wet deposition and PECVD).

The successful depositions of the blocking agents were confirmed by comparison of the wettability and the morphology of the PMMA sheets deposited with BSA, DOTAP, wet DEGDME and dry DEGDME and with those of oxygen plasma treated (PT) and plain PMMA sheets (**Fig. 2**). The differences in contact angles are attributed to the nature of the surface-exposed chemical groups after the depositions. The contact angle  $70^\circ$  of plain PMMA was slightly reduced after it was deposited with BSA or DOTAP (**Fig. 3**). We reason that the deposition mechanism for DOTAP involves adsorption of DOTAP's hydrophobic tail onto the PMMA surface thus exposing the trimethyl-amine 'head' along with the polar ester groups. BSA on the other hand might adsorb in layers, in which the BSA molecules at the bottom change their conformation, exposing some of the hydrophobic amino acids to make good contact with the PMMA. Another layer(s) of BSA might then adsorb on it, mainly through protein-protein interactions. The PMMA water contact angle dropped significantly after the deposition of wet and dry DEGDME as well as of PT PMMA. The largest drop is seen after the dry DEGDME deposition which brings the contact angle down to  $35^\circ$  (**Fig. 3**). It should be noted that the composition of the dry DEGDME is different from that of the wet DEGDME. The wet DEGDME film contains unfragmented DEGDME molecules whereas the dry DEGDME film is composed of an underlying TEOS layer and cross-linked DEGDME molecules. The very low water contact angle of the dry DEGDME PMMA sheet is suggesting that TEOS might be inserted into the DEGDME layer and an effective plasma polymerization had taken place. In general, plasma treatment leads to fragmentation of the DEGDME precursor, thus some charged residues (with  $-O^-$  group) and hydroxyl groups are likely to be formed. The hydrophilic nature of this surface is also explained by the presence of the silanols (from TEOS), although we can only speculate whether such groups are available on the top surface or are embedded in the bulk layer. Similar fragmentation effect could also be seen on the plasma treated PMMA slide. Presumably, some of the methyl esters are oxidized into carboxylic acids. Other highly reactive species might appear too, such as oxygen radicals and anions. However, they are highly reactive and unstable for longer period of time. The morphologies of PMMA sheets deposited with different blocking agents were also shown in **Fig. 4**. The plain PMMA surface is not smooth with scattered craters throughout (**Fig. 4(c)**). However, after BSA deposition, the craters on the surface have been filled with BSA and the surface become uneven (**Fig. 4(a)**). The coating of DOTAP on PMMA made the surface become slightly evenner thank to the filling of DOTAP into the craters (**Fig. 4(b)**). After deposition with wet DEGDME, the surface become more wavy and uneven as seen in the case of BSA deposition (**Fig. 4(e)**). However, of all the deposition method, the sequential deposition of TEOS and DEGDME on the PT PMMA resulted in the roughest surface as seen in **Fig. 4(f)**. Interestingly, the dry DEGDME film is the only film, roughness of which can further increase upon contact with water (data not shown) due to its swelling properties. This surface becomes very well hydrated thus resembling a structure of hydrogels. We therefore believe that it is not the roughness but the vast hydration that is the dominant factor responsible for its increased protein repellent properties.

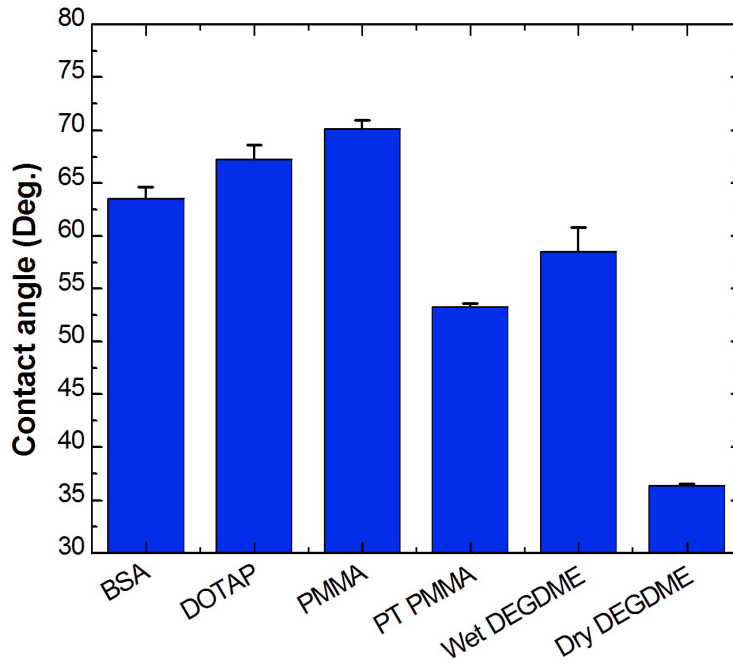


**Fig. 3.** Water contact angles measured on PMMA sheets coated with different blocking agents. As a comparison, water contact angle of the plain PMMA and PT PMMA were also shown. While coatings of BSA and DOTAP result in small changes in water contact angle, plasma treated and wet DEGDM coating result in significant change in the contact angle. However, the dry DEGDM coating gave the highest reduction in water contact angle. Note that dry DEGDM coating is different from wet DEGDM coating, an underneath TEOS matrix might have contributed to this difference.

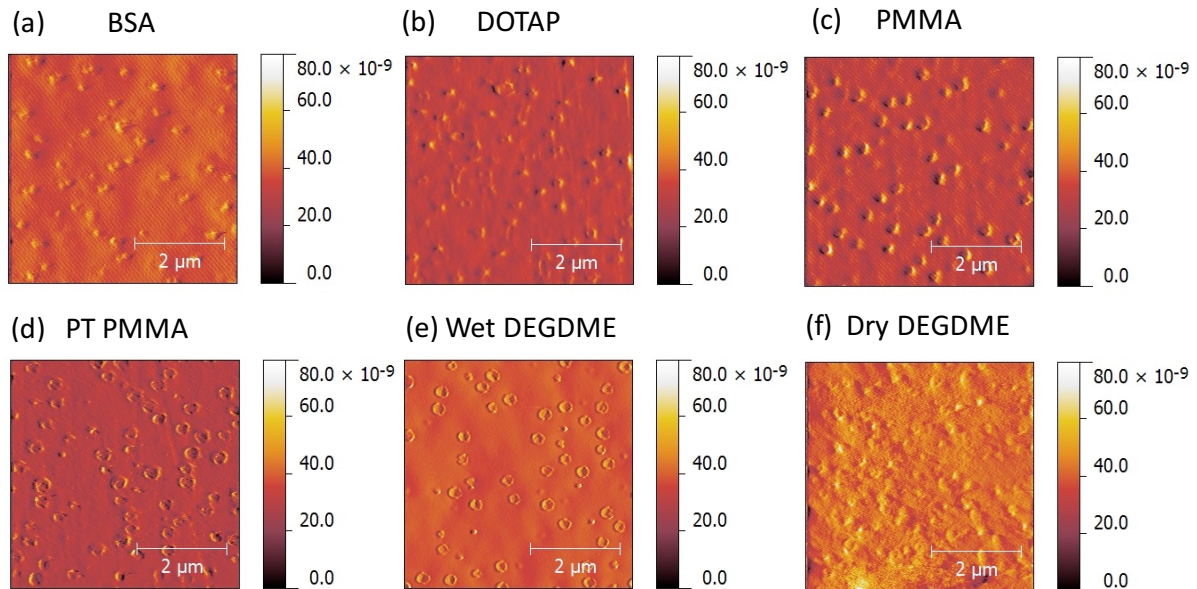


**Fig. 4.** AFM images in contact mode of PMMA sheets deposited with different blocking agent: (a) BSA (RMS =  $9.62 \pm 2.58$  nm), (b) DOTAP (RMS =  $4.49 \pm 0.09$  nm), (e) wet DEGDM (RMS =  $16.63 \pm 3.17$  nm) and (f) dry DEGDM (RMS =  $21.1 \pm 9.46$  nm). For comparison, the AFM image of plain and PT PMMA surface were also shown in (c) (RMS =  $4.06 \pm 0.50$  nm) and (d) (RMS =  $3.56 \pm 0.62$  nm), respectively. The AFM surface topologies together with the water contact angle data in Fig. 3 clearly confirm the successful coatings of BSA, DOTAP, wet and dry DEGDM onto PMMA surface.

### 3.2 Blocking effects measured by fluorescence microscopy

The fluorescent images of the reaction well of the blocking agent deposited PMMA flow-cell deposited with Cy5-labelled anti-IgG were shown in **Fig. 5(a-f)**. The rectangular areas of  $500\ \mu\text{m} \times 1000\ \mu\text{m}$  in the expanded regions of the PMMA microwells were used to measure the mean and the standard deviation of fluorescent intensities. The Cy5-labelled anti-IgG adsorbed to plain PMMA microwell showed very uneven fluorescent intensity. It could be speculated that the protein anti-IgG were absorbed randomly depending on their preferences toward the hydrophobic PMMA surface. Of all the blocking agents, the DOTAP resulted in the most uniform blocking as shown in **Fig. 5(b)**. The BSA and dry DEGDME also resulted in a relatively good and uniform blocking. The fluorescent intensity measurements inside the rectangular areas were shown in **Fig. 6** confirmed the observation from fluorescent images in **Fig. 5**. The fluorescent intensity of the absorbed Cy5-labelled anti-IgG onto the DOTAP blocked PMMA microwell showed the smallest value. On the other hand, without blocking, the fluorescent intensity was the highest and very non-uniform. The blocking of BSA is as good as that of dry DEGDME. BSA is widely used for blocking the non-specific adsorption of proteins [29], with typical concentrations ranging from 0.5 – 3 % w/w. Interestingly, the cationic DOTAP showed very good blocking with respect to protein non-specific adsorption. The blocking effect of DOTAP has been shown previously inside fused silica capillary [30] but it is the first time it has been shown here to significantly reduce the nonspecific adsorption of proteins onto PMMA surface. Both the BSA and the DOTAP films represent examples where the predominant forces responsible for the low protein adsorption are based on electrostatic interactions. Such repulsive (or attractive) forces can be relatively easily tuned to repel specific proteins by adjusting the pH of the solution above (or below, depending on the charge of the modified PMMA surface) the isoelectric point of the given protein. The repulsion of proteins by PEG-like materials from DEGDME is also in agreement with previous work [32]. However, it is interesting to note that the dry DEGDME prepared by PECVD showed superior blocking performance compared to that of wet DEGDME. Moreover, the blocking from wet DEGDME is not uniform inside the microwell. It could be due the fact that in wet DEGDME film, only the DEGDME molecules were simply adsorbed onto the activated PMMA surface while for the dry DEGDME film, an intermediate TEOS layer was inserted and formed a robust scaffold for the DEGDME to be built on. The PT PMMA surface showed relatively uniform adsorption of proteins in contrast to the plain PMMA surface. It has been shown previously that the oxygen plasma treatment created carboxylic groups and other reactive radicals on the PMMA surface which could allow the binding of the proteins [35].

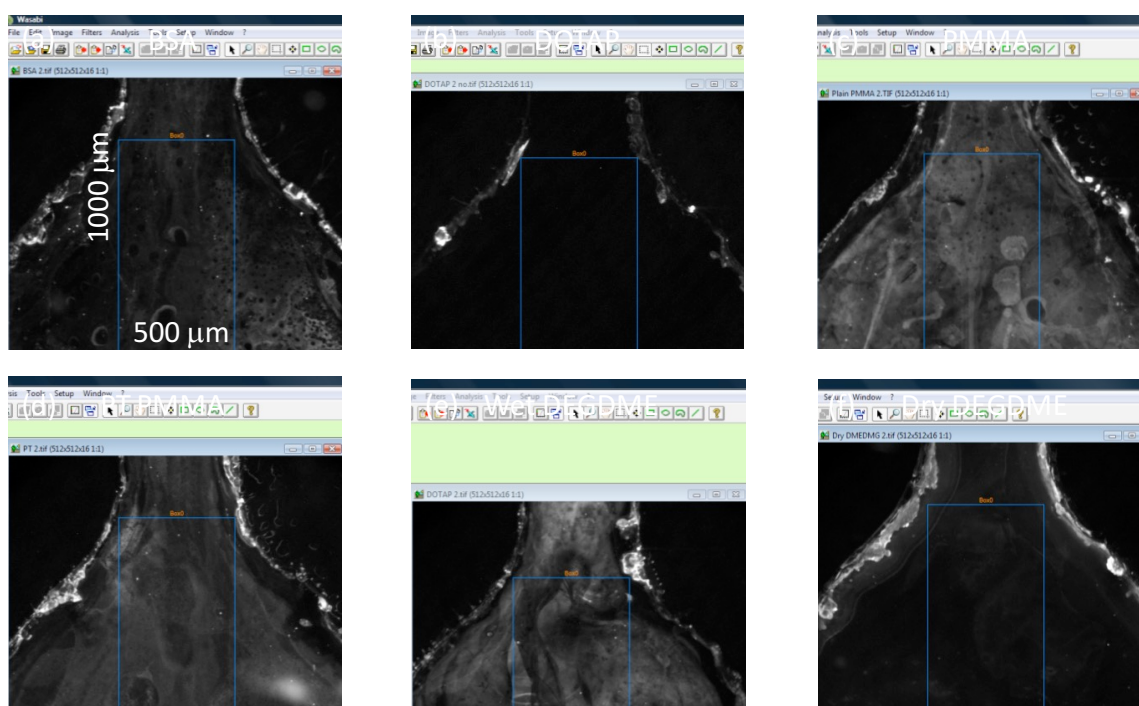


**Fig. 5.** Fluorescent images on the reaction chambers of the flow-cell deposited with Cy5-anti-IgG (25  $\mu\text{g/ml}$ ) after 60 min of reaction on: (a) BSA, (b) DOTAP, (e) wet DEGDME and (f) dry DEGDME coatings, respectively. For comparison, the fluorescent images of the same regions on the plain and PT PMMA flow-cell were shown in Fig. 5(c) and (d), respectively. As can be seen, the DOTAP and dry DEGDME not only suppress the non-specific binding of Cy5-anti-IgG effectively but also uniformly across the reaction chambers. On the other hand, the Cy5-anti-IgG bind very randomly to the plain PMMA and wet DEGDME coatings resulting in highly non-uniform fluorescent intensity across the reaction chambers.

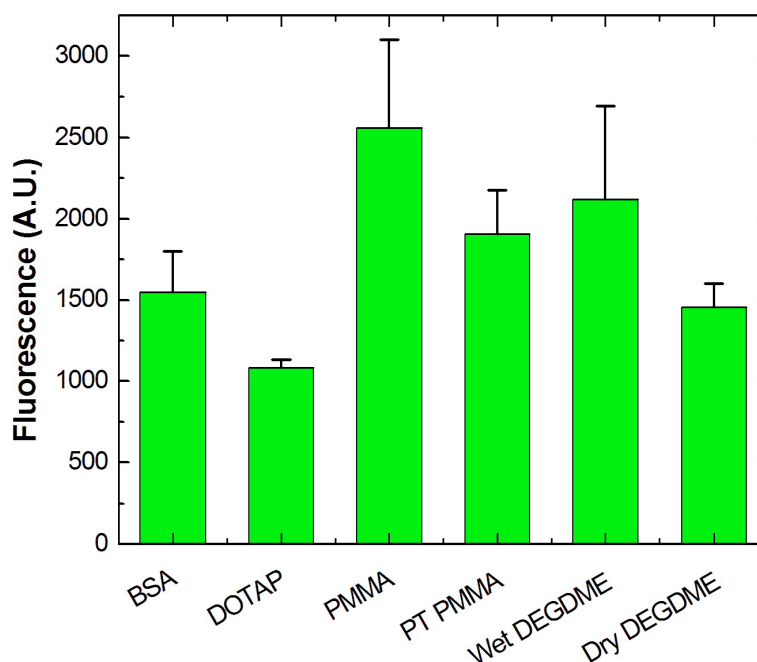


**Fig. 6.** Fluorescent intensities measured on the rectangular areas indicated in Fig. 5 of PMMA flow-cells deposited with 30  $\mu\text{l}$  of Cy5-labelled anti-IgG with concentrations of 25  $\mu\text{g/ml}$  in PBS (pH 7.4). The error bars represent the standard deviations of the fluorescent intensities of the pixels inside the rectangular areas. This result again confirms the superiority of DOTAP and dry DEGDME coatings compared to the remaining coatings for blocking Cy5-labelled anti-IgG non-specific binding onto PMMA surface.

### 3.3 Stability of blocking agents and their effects on subsequent anti- $\alpha$ -hCG adsorption assay

The  $\Psi$  and  $\Delta$  spectra measured on the Au-coated surface after rinsing the blocking agent-coated PMMA flow-cells with PBS buffer in 15 min and subsequent adsorption of anti- $\alpha$ -hCG in 60 min were shown in **Fig. 7(a-e)**. Since it is not possible to perform TIRE measurements without the presence of aqueous buffer inside the microwells, the first set of  $\Psi$  and  $\Delta$  spectra reflected not only the Au film but also any materials that could be removed from the PMMA flow-cell and deposited onto the Au surface after rinsing with PBS in 15 min [17]. The SPR wavelength of the first set of spectra was varied from well to well since the optical alignment and the thickness of the organic materials deposited from the PBS rinsing might be different. Nevertheless, the SPR wavelength was centred around 700 nm. After the first set of  $\Psi$  and  $\Delta$  spectra, the second set of  $\Psi$  and  $\Delta$  spectra corresponding to the adsorption of 50  $\mu\text{g/ml}$  of anti- $\alpha$ -hCG to the contaminated Au sensing surface showed different shifts from microwell to microwell. For the DOTAP and BSA-coated microwells, the relative shifts are very small from the first  $\Psi$  and  $\Delta$  spectra. We reasoned that some of the DOTAP and BSA might have been removed from the PMMA flow-cell and deposited back onto the Au surface thus blocking the subsequent binding of the anti- $\alpha$ -hCG. Accordingly, this resulted in very small shift in the  $\Psi$  and  $\Delta$  spectra. For the remaining plain, PT, wet and dry DEGDME-coated microwells, the shifts were very distinctive and large meaning a large amount of anti- $\alpha$ -hCG has been deposited onto the contaminated Au sensing surface.

Fitting results of the first  $\Psi$  and  $\Delta$  spectra to a four-layer model resulted in thickness of organic materials being deposited onto the Au surface after rinsing with PBS after 15 min (**Fig. 8**). The results indicate that BSA and DOTAP have been desorbed from BSA and DOTAP-coated microwells, respectively, and being deposited back on the sensing Au surface. Despite that the DOTAP film deposited onto PMMA surface has been shown to have very good protein blocking performance, this cationic lipid appears not to be very stable in aqueous environment as has been shown in the case of DODAB film [36]. It seems that the cumulative effect of the Van der Waals forces between the hydrophobic chain of DOTAP and the methoxy groups of PMMA is not strong enough for longer their adhesion under aqueous conditions. Similarly, the BSA film was also formed by physical adsorption of BSA onto the PMMA microwells thus some loosely bound BSA might have also been removed due to the rinsing with PBS. The dimensions of BSA are  $14 \times 4 \times 4 \text{ nm}^3$ . The DOTAP molecule is composed of the hydrophobic part of the lipid which is  $\sim 2.1 \text{ nm}$  in size and the hydrophilic part which is another  $\sim 1 \text{ nm}$  in size. From the ellipsometric fitting in **Fig. 8** and size of BSA and DOTAP molecules, it is likely that a monolayer of BSA (lying flat) and DOTAP have been re-adsorbed onto the Au surface. It is interesting to note that the wet DEGDME also showed a relatively large thickness of organic layer deposited. It could be explained by the fact that the DEGDME has only been dynamically coated onto the PT PMMA surface, thus some loosely bound DEGDME might have been removed and deposited back to Au surface. The plain, PT PMMA and dry DEGDME-coated microwells showed a very thin layer of organic materials deposited onto the Au surface, confirming their stability and resistance against washing in buffered solution. The small amount of deposited organic material could come from the dirt or salt inside the PBS buffer being used. Overall, the dry DEGDME film, covalently cross-linked with siloxane (TEOS) is very robust under the rinsing of PBS flow inside the microwell compared to other coatings.

The increases in the thickness after adsorption of anti- $\alpha$ -hCG onto the Au sensing substrate was shown in **Fig. 9**. We observed a small thickness increment after adsorption of anti- $\alpha$ -hCG onto the contaminated Au sensing surface inside the DOTAP and BSA-coated microwells. Whereas the remaining four microwells including plain, PT, wet and dry DEGDME showed good adsorption of the protein onto the Au surface, meaning the thickness increments are large. Finally, the kinetic data of the change in  $\Psi$  and  $\Delta$  from the PBS rinsing to the introduction of  $\alpha$ -anti-hCG showed convincing data about the effect the blocking of the Au surface by the removed blocking agents on the kinetic of the adsorption of the protein (**Fig. 10**). In BSA and DOTAP-coated microwells, the  $\Psi$  and  $\Delta$  response were very slow after the introduction of the protein solution, i.e. the contaminated Au surface of the sensing substrate has been partially blocked thus reducing the rate of adsorption of the proteins. On the other hand, the adsorption happened very fast, i.e. within 30 to 40 s, on the PMMA microwells blocked by wet and dry DEGDME as well as in the plain and PT PMMA microwells. This is strongly supporting our hypothesis about the effect of the desorption of blocking agents with respect to the subsequent assays which are based-on the adsorption of anti- $\alpha$ -hCG onto the Au sensing substrates. We expect this finding would be useful to be considered when blocking PMMA-based biosensor devices with non-specific adsorption blocking agents [22-26].

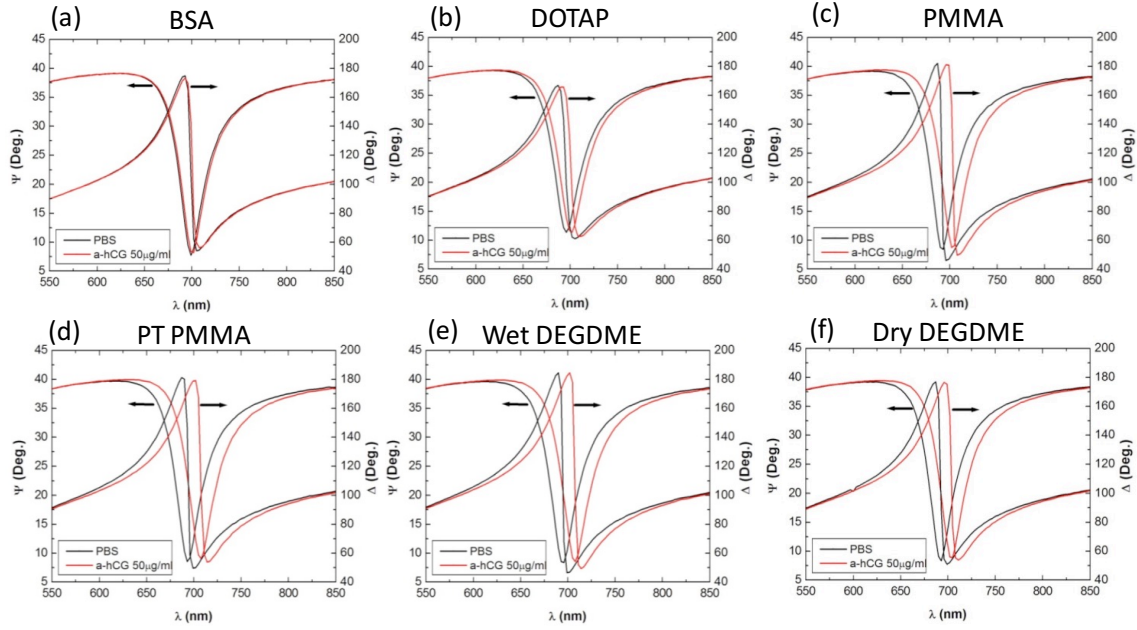


**Fig. 7.**  $\Psi$  and  $\Delta$  spectral shifts after adsorption of anti- $\alpha$ -hCG 50  $\mu$ g/ml in 60 min to Au-coated glass sensing substrate in PMMA microwells blocked with (a) BSA, (b) DOTAP, (e) Wet DEGDM and (f) dry DEGDM. For comparison, the spectral shifts in plain and PT PMMA microwells were also shown in (c) and (d), respectively. Note that the PBS spectra in all figures do not represent PBS buffer on plain gold surfaces but they represent PBS buffer on contaminated gold surfaces deposited with any organic materials removed from rinsing of the coatings with PBS buffer in 15 min at 5  $\mu$ l/min.

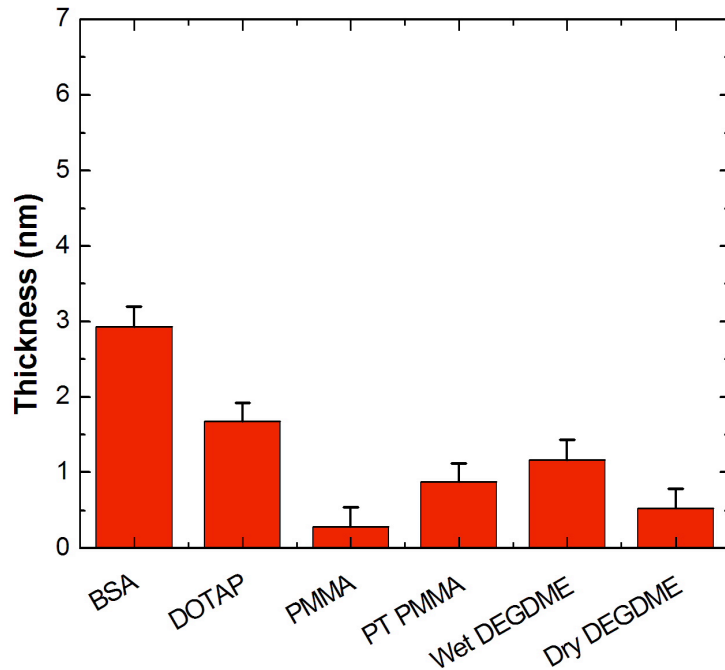


**Fig. 8.** Thickness of organic layer removed from the coating materials and deposited back onto the Au surface after rinsing the microwells with PBS buffer in 15 min at flow rate of 5  $\mu$ l/min. A four-layer ellipsometric model was used in the fitting with the PsiDelta 2 software (Jobin Yvon Horiba, France) to estimate the thickness of the organic layer. A Cauchy dispersion formula  $A + B/\lambda^2 + C/\lambda^4$  where  $A = 1.415$ ,  $B = 0.01 \text{ nm}^2$  and  $C = 0$  was used to model the refractive indices of all organic layers with the assumption that the difference in their refractive

indices is negligible [21]. In this case, the larger the thicknesses (e.g. BSA and DOTAP), the less stable the corresponding coatings against buffer washing.

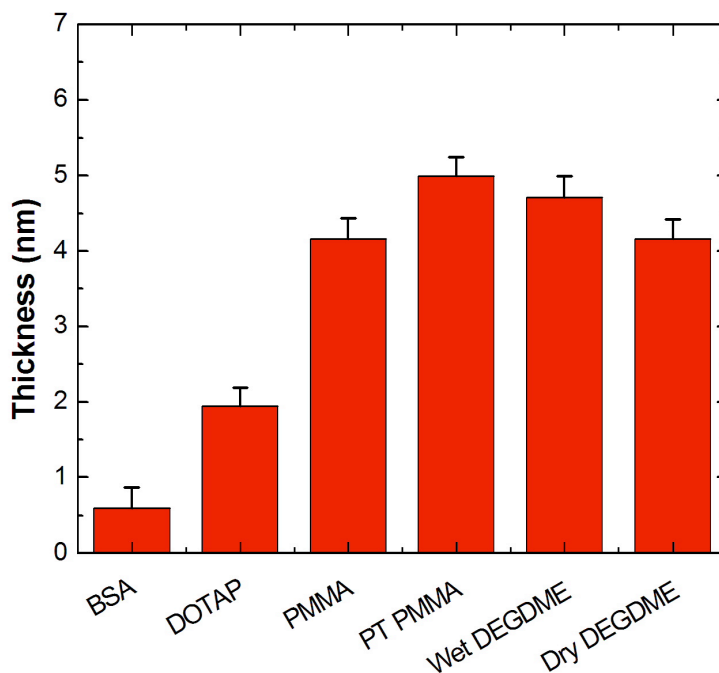


**Fig. 9.** Thicknesses of anti- $\alpha$ -hCG at 50  $\mu$ g/ml deposited onto contaminated Au surfaces in different microwells after 60 min of reaction. Here, contaminated Au surfaces are Au surfaces deposited with organic layers removed from the coatings. These thicknesses of anti- $\alpha$ -hCG were obtained by subtracting the absolute thicknesses from the ellipsometric fitting to the thicknesses of the organic layers in Fig. 8 [21]. In this case, anti- $\alpha$ -hCG physisorbed very less to the Au surfaces contaminated with BSA and DOTAP removed from the coatings.

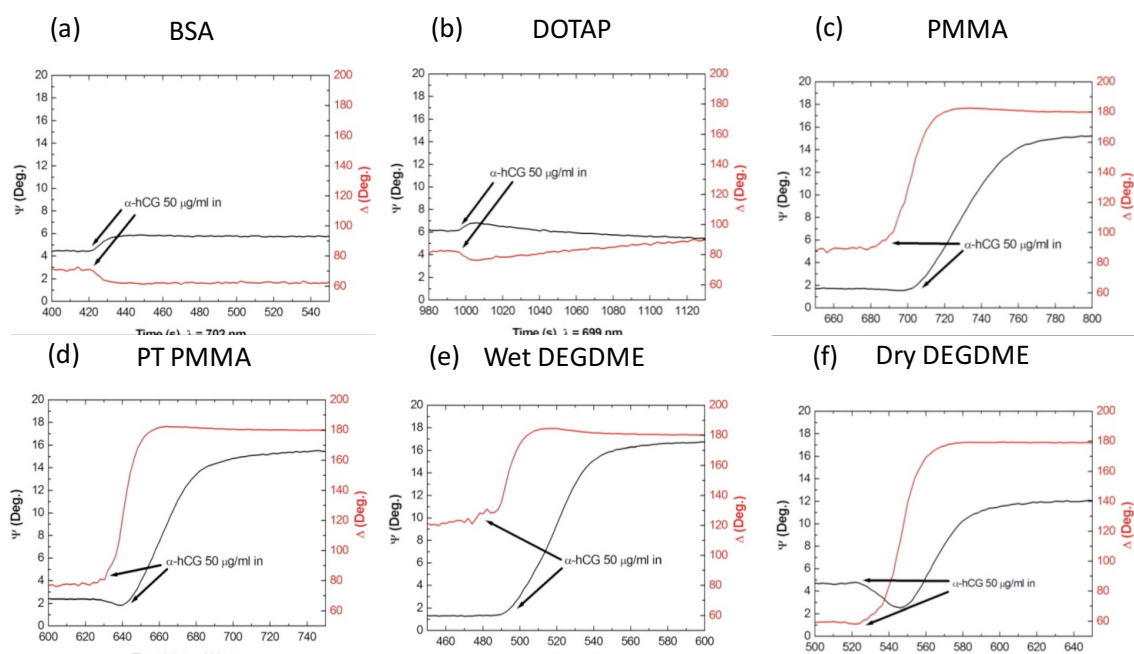


**Fig. 10.** The effect of the instability of the coatings were further manifested by looking at the kinetics of  $\Psi$  and  $\Delta$  measured on the Au substrates before and after injection of anti- $\alpha$ -hCG at 50  $\mu$ g/ml in different PMMA microwells blocked with (a) BSA, (b) DOTAP, (e) wet DEGDME and (f) dry DEGDME. For comparison, the kinetics of  $\Psi$  and  $\Delta$  in plain and PT PMMA microwells were also shown in (c) and (d), respectively. For

DOTAP and BSA coatings, the Au surfaces have been blocked by a layer of DOTAP and BSA removed from the PMMA surfaces of the microwells thus preventing the physisorption of anti- $\alpha$ -hCG (i.e. the rates change of  $\Psi$  and  $\Delta$  are very slow compared to other coatings). The flow-rate of the syringe pump was adjusted at 5  $\mu$ l/min. The kinetic wavelength was chosen to maximize the change in  $\Psi$  and  $\Delta$  signal.

#### 4. Conclusions

A comprehensive comparison of different surface coatings for suppression of non-specific adsorption on PMMA surfaces has been carried out. Measurements using WCA and AFM confirmed the successful modification of the PMMA surfaces with blocking agents. Fluorescent measurements show that the DOTAP is the best of all the coatings tested to suppress the non-specific binding of Cy5-labelled anti-IgG onto the PMMA surface. BSA and plasma deposited dry DEGDME coatings also showed very good suppression of non-specific adsorption of proteins. However, results obtained from TIRE showed that DOTAP and BSA could be removed from PMMA surfaces upon rinsing with PBS buffer and deposited back to Au sensing substrate. The deposition of the blocking agents onto Au sensing substrate was manifested in the kinetics and the amounts of the adsorbed anti- $\alpha$ -hCG proteins. Overall, the dry DEGDME coating deposited by PECVD showed very good blocking and excellent stability when rinsing with PBS buffer. Our results could be useful when one considers blocking agents to suppress the non-specific adsorption of analyte inside PMMA devices. In particular, it would have implications on PMMA-based biosensor devices integrated with sensing elements for electrochemical or optical detections.

#### Acknowledgements

This material is based upon work supported by the Science Foundation Ireland under Grant No. SFI/10/CE/B1821. D. E. Williams is an E.T.S. Walton Visiting Fellow of Science Foundation Ireland.

#### References

- [1] Reyes D. R., Iossifidis D., Aurox P.-A., Manz A. "Micro total analysis systems. 1. Introduction, theory, and technology" *Anal. Chem.* **74**, 2623-2636, 2002
- [2] Aurox P.-A., Iossifidis D., Reyes D. R., Manz A. "Micro total analysis systems. 2. Analytical standard operations and applications" *Anal. Chem.* **74**, 2637-2652, 2002
- [3] Dittrich P. S., Tachikawa K., Manz A. "Micro total analysis systems. Latest advancements and trends" *Anal. Chem.* **78**, 3887-3908, 2006
- [4] J. West, M. Becker, S. Tombrink and A. Manz "Micro total analysis systems: Latest achievements" *Anal. Chem.* **80**, 4403-4419, 2008
- [5] Marie R., Beech J. P., Voros J., Tegenfeldt J. O., Hook F., Use of PLL-g-PEG in micro-fluidic devices for localizing selective and specific protein binding, *Langmuir*, 2006, 22, 10103-10108
- [6] Liu J., Lee M. L., Permanent surface modification of polymeric capillary electrophoresis microchips for protein and peptide analysis, *Electrophoresis*, 2006, 27, 3533-3546
- [7] Bi H., Meng S., Li Y., Guo K., Chen Y., Kong J., Yang P., Zhong W., Liu B., Deposition of PEG onto PMMA microchannel surface to minimize nonspecific adsorption, *Lab Chip*, 2006, 6, 769-775
- [8] Muck A., Svatoš A., Chemical modification of polymeric microchip devices, *Talanta*, 2007, 74, 333-341
- [9] Lin Y.W., Chang H.T., Modification of poly(methyl methacrylate) microchannels for highly efficient and reproducible electrophoretic separations of double-stranded DNA, *J. Chromatogr. A*, 2005, 1073, 191-199

- [10] Dang F., Kakehi K., Cheng J., Tabata O., Kurokawa M., Nakajima K., Ishikawa M., Baba Y., Hybrid Dynamic Coating with *n*-Dodecyl  $\beta$ -D-Maltoside and Methyl Cellulose for High-Performance Carbohydrate Analysis on Poly(methyl methacrylate) Chips, *Anal. Chem.*, 2006, 78, 1452-1458
- [11] Mohamadi M. R., Mahmoudian L., Kaji N., Tokeshi N., Baba Y., Dynamic coating using methylcellulose and polysorbate 20 for nondenaturing electrophoresis of proteins on plastic microchips, *Electrophoresis*, 2007, 28, 830-836
- [12] Lai S., Cao X., Lee L. J., A packaging technique for polymer microfluidic platforms, *Anal. Chem.*, 2004, 76, 1175-1183
- [13] Liu J., Pan T., Woolley A. T., Lee M. L., Surface-modified poly(methyl methacrylate) capillary electrophoresis microchips for protein and peptide analysis, *Anal. Chem.*, 2004, 76, 6948-6955
- [14] Westphal P., Bornmann A., Biomolecular detection by surface plasmon enhanced ellipsometry, *Sens. Actuators B*, 2002, 84, 278– 282.
- [15] Arwin H., Poksinski M., Johansen K., Total internal reflection ellipsometry: principles and applications, *Appl. Opt.* 2004, 43, 3028–3036.
- [16] Poksinski M., Arwin H., Protein monolayers monitored by internal reflection ellipsometry, *Thin Solid Films*, 2004, 455–456C, 716–721
- [17] Poksinski M., Arwin H., Total internal reflection ellipsometry: ultrahigh sensitivity for protein adsorption on metal surfaces, *Opt. Lett.*, 2007, 32, 1308-1310
- [18] Nabok A., Tsargorodskaya A., Hassan A.K., Starodub N.F., Total internal reflection ellipsometry and SPR detection of low molecular weight environmental toxins, *Appl. Surf. Sci.* 2005, 246, 381–386.
- [19] Nabok A., Tsargorodskaya A., Davis F., Higson S.P.J., The study of genomic DNA adsorption and subsequent interactions using total internal reflection ellipsometry, *Biosens. Bioelectron.*, 2007, 23, 377–383.
- [20] Nabok A, Tsargorodskaya A., Holloway A, Starodub N. F., and Demchenko A., Specific binding of large aggregates of amphiphilic molecules to the respective antibodies, *Langmuir*, 2007, 23, 8485-8490
- [21] Le N. C. H., Gubala V., Gandhiraman P. R., Coyle C., Daniels S., Williams D. E., Total internal reflection ellipsometry (TIRE) as a label-free assessment method for optimisation of the reactive surface of bioassay devices based on a functionalized cyclo olefin polymer, *Anal. Bioanal. Chem.*, 2010, 398, 1927-1936
- [22] Qi S., Liu X., Ford S., Barrows J., Thomas G., Kelly K, McCandless A, Lian K., Goettert J., Soper S. A., Microfluidic devices fabricated in poly(methyl methacrylate) using hot-embossing with integrated sampling capillary and fiber optics for fluorescence detection, *Lab Chip*, 2002, 2, 88–95
- [23] Horng R. H., Han P., Chen H. Y., Lin K. W., Tsai T. M., Zen J. M., PMMA-based capillary electrophoresis electrochemical detection microchip fabrication, *J. Micromech. Microeng.*, 2005, 15, 6–10
- [24] Bai Y., Koh C. G., Boreman M., Juang Y., Tang I., Lee L. J., Yang S., Surface modification for enhancing antibody binding on polymer-based microfluidic device for enzyme-linked immunosorbent assay, *Langmuir*, 2006, 22, 9458-9467
- [25] Nugen S.R., Asiello P. J., Connelly J. T., Baeumner A. J., PMMA biosensor for nucleic acids with integrated mixer and electrochemical detection, *Biosens. Bioelectron.*, 2009, 24, 2428–2433
- [26] Baldini F., Carloni A., Giannetti A., Porro G., Trono C., An optical PMMA biochip based on fluorescence anisotropy: Application to C-reactive protein assay, *Sens. Actuators B*, 2009, 139, 64-68

- [27] Hamada K., Yamashita K., Serizawa T., Kitayama T., Akashi M., Adsorption of bovine serum albumin onto poly(methyl methacrylate) stereocomplex films with a molecularly regulated nanostructure, *J. Polym. Sci., Part A: Polym. Chem.*, 2003, 41, 1807-1812
- [28] Tsougeni K., Petrou P. S., Tserepi A., Kakabakos S. E., Gogolides E., Nano-texturing of poly(methyl methacrylate) polymer using plasma processes and applications in wetting control and protein adsorption, *Microelectron. Eng.* 2009, 86, 1424–1427
- [29] Jensen J., Hoiby P., Emiliyanov G., Bang O., Pedersen L., Bjarklev A., Selective detection of antibodies in microstructured polymer optical fibers, *Opt. Express*, 2005, 13, 5883-5889
- [30] Bonoli M., Varjo S. J.O., Wiedmer S. K., Riekkola M.-L., Cationic lipid vesicles as coating precursors in capillary electrochromatography: Separation of basic proteins and neutral steroids, *J. Chromatogr. A*, 2006, 1119, 163–169
- [31] Sardella E., Gristina R., Senesi G. S., d'Agostino R., Favia R., Homogeneous and micro-patterned plasma-deposited PEO-like coatings for biomedical surfaces, *Plasma Process. Polym.*, 2004, 1, 63–72
- [32] Valsesia A., Colpo A., Meziani T., Bretagnol F., Lejeune M., Rossi F., Bouma A., Garcia-Parajo M., Selective immobilization of protein clusters on polymeric nanocraters, *Adv. Funct. Mater.*, 2006, 16, 1242–1246
- [33] Belegirinou S., Mannelli I., Lisboa P., Bretagnol F., Valsesia A., Ceccone G., Colpo P., Rauscher H., Rossi F., pH-dependent immobilization of proteins on surfaces functionalized by plasma-enhanced chemical vapor deposition of poly(acrylic acid)-and poly(ethylene oxide)-like films, *Langmuir*, 2008, 24, 7251-7261
- [34] Gandhiraman R.P., Karkari S.K., Daniels S.M., MacCraith B.D., Influence of ion bombardment on the surface functionalization of plasma deposited coatings, *Surf. Coat. Tech.*, 2009, 203, 3521- 3526.
- [35] Brown L., Koerner T., Horton J. H., Oleschuk R. D., Fabrication and characterization of poly(methylmethacrylate) microfluidic devices bonded using surface modifications and solvents, *Lab Chip*, 2006, 6, 66-73
- [36] Pereira E. M. A., Kosaka P. M., Rosa H., Vieira D. B., Kawano Y., Petri D. F. S., Carmona-Ribeiro A. M., Hybrid materials from intermolecular associations between cationic lipid and polymers, *J. Phys. Chem. B* 2008, 112, 9301–9310